Fully Nonlinear Statistics of Wave Crest Elevation Calculated Using a Spectral Response Surface Method: Applications to Unidirectional Sea States

R. S. GIBSON AND C. SWAN

Department of Civil and Environmental Engineering, Imperial College London, London, United Kingdom

P. S. TROMANS

Ocean Wave Engineering, Ltd., Liss, Hampshire, and Department of Civil and Environmental Engineering, Imperial College London, London, United Kingdom

(Manuscript received 16 June 2005, in final form 3 January 2006)

ABSTRACT

This paper concerns the calculation of the probability of exceedance of wave crest elevation. The statistics have been calculated for broadbanded, unidirectional, deep-water sea states by incorporating a fully nonlinear wave model into a spectral response surface method. This is a novel approach to the calculation of statistics and, as all of the calculations are performed in the probability domain, avoids the need for long time-domain simulations. Furthermore, in contrast to theoretical distributions, the broadbanded, fully nonlinear nature of the sea state can be considered. The results have been compared with those of fully nonlinear time-domain simulations and are shown to be in good agreement. The results indicate that in unidirectional seas the crest elevations of the largest waves can be much higher than would be predicted by linear or second-order theory. Hence, the occurrence of locally long crested sea states offers a possible explanation for the formation of freak or rogue waves.

1. Introduction

The statistics of wave crest elevation are fundamental to the design of both deep-water offshore structures and shallow-water coastal structures. In the case of fixed structures, deck elevations are typically set to maintain an effective air gap, thereby preventing the impact of the largest wave crests on the underside of the structure. In addition, individual members must be designed to support the applied loads, with the maximum drag forces arising beneath the largest wave crests and being proportional to the square of the wave amplitude. For floating structures the occurrence of wave slamming, the extreme vessel response (particularly roll motion), and green-water inundation are all key parameters dependent upon extreme wave events. Likewise, crest elevations represent a key point in the design of coastal structures, both fixed and floating, for shoreline protection and flood prevention. In the latter some degree of overtopping must be anticipated, but its estimation should be based upon a clear understanding of crest-height distributions.

This paper is concerned with the calculation of the exceedance probability of wave crest elevation, in deep water, in unidirectional seas. Directionally spread wave fields will be considered in a future paper. The statistical distributions have been calculated using two recent advances in wave modeling. The first concerns the fully nonlinear wave model proposed by Bateman et al. (2001, hereinafter referred to as BST), while the second involves the use of a spectral response surface (SRS) method, which was not developed in the context of wave modeling, but can be very usefully applied therein. For example, Tromans and Vanderschuren (2004) have previously used the method, in conjunction with the wave model proposed by Sharma and Dean (1981), to calculate the probability of exceedance of crest elevation to second order, and the results have been shown to be in excellent agreement with those of the second-order time-domain simulations of Forristall (2000).

Within the present paper the application of the BST model within the SRS method provides a first oppor-

Corresponding author address: C. Swan, Department of Civil and Environmental Engineering, Imperial College London, London SW7 2AZ, United Kingdom.
E-mail: c.swan@imperial.ac.uk

DOI: 10.1175/JPO2956.1

tunity to calculate statistical distributions in which the full nonlinearity of an evolving (unsteady) wave field are included. The motivation for undertaking this task is twofold. First, the ongoing discussion of freak or rogue waves frequently implies that the description of the largest or steepest waves may include significant contributions from third- and higher-order interactions. Second, recent calculations of large isolated wave groups (Gibson and Swan 2007, hereinafter GS) have shown that the resonant, and near-resonant, interactions arising at third-order can produce local, and rapid, changes to the spectrum of the freely propagating wave components. In unidirectional seas this involves a broadening of the underlying spectrum, providing the potential for larger maximum crest elevations to evolve.

The paper begins in section 2 by describing the background to the calculations, together with a brief overview of the BST model. It continues in section 3 by describing the application of the SRS method, and in section 4 the method is applied to calculate the probability of exceedance of crest elevation in two unidirectional sea states. These results are compared with those of fully nonlinear, random, time-domain simulations in section 5, with concluding remarks provided in section 6.

2. Background

Although there is generally good agreement between observed and theoretical crest elevations, there is some suggestion of the existence of freak, or rogue, waves that are much higher and steeper than might be expected (e.g., Sand 1990). The exact definition of what constitutes a rogue wave remains the subject of much debate; however, it is broadly agreed that the occurrence of such waves cannot be predicted using second-order theory. Therefore, one limitation of theoretical distributions is that they do not consider the full nonlinearity of the wave field. Another is that most do not take into account the broadbanded nature of the ocean environment, both in terms of a realistic wave spectrum and also in terms of the directional spread of the wave energy. In contrast, time-domain simulations are a robust method for determining statistical distributions. Indeed, rogue waves apart, the statistics derived from the second-order time-domain simulations of Forristall (2000) have been found to be in good agreement with measured data. However, in order to have confidence in the extremes of the distributions, many hours of a particular sea state must be modeled.

Many of these limitations can be overcome by using the SRS method. First, by incorporating a suitable wave model into the method, the full nonlinearity can be considered. This task is addressed in the present paper. Second, the sea state can be described by a realistic broadbanded and directionally spread spectrum; the former is addressed herein, and the latter is left for a subsequent paper for reasons that will become apparent. Furthermore, the property of the wave field that is of interest can be expressed in either the time domain (e.g., wave height) or the frequency domain (e.g., crest elevation). One final advantage is that it takes the same length of time to determine the extremes of a distribution as it does any other part. However, the SRS method also has two important limitations. First, in order to calculate the probability of exceedance of a certain response (be it crest elevation or wave height), a constrained optimization problem must be solved. The difficulty lies in the fact that in many cases the function to be optimized is not only nonlinear, but may also contain several local maxima. As a result, particular attention must be given to the solution of this constrained optimization problem. Second, the shape of the response surface is unknown and must be approximated. This is undertaken through the Taylor series expansion of the response surface about the point with the greatest probability density. In a first-order reliability method (or FORM) this approximation is linear, while in a second-order reliability method (or SORM) it is parabolic. Both approximations are considered in the present paper and are described in more detail in section 3.

Before considering the details of the SRS method, it is appropriate to briefly review the BST model. This wave model represents a recent contribution to a class of wave solutions, first envisaged by Zakharov (1968), in which a spatial description of the water surface elevation, $\eta\,(x, y)$, and the velocity potential on that surface, $\phi\,(x, y, \eta)$, are time marched using the nonlinear kinematic and dynamic free-surface boundary conditions. In applying solutions of this type, the fluid is assumed to be inviscid and incompressible, and the wave-induced motion irrotational. Based on these assumptions, the BST model provides a fully nonlinear description of the evolution of large waves in realistic wave fields, involving a significant spread of energy in both frequency and direction. In practice, the wave model may be subdivided into two parts. The first, full details of which are given in Bateman et al. (2001), concerns the evolution of the water surface elevations, η, and is directly relevant to the present application, while the second, described in a follow-up paper (Bateman et al. 2003) adopts a related approach to the description of the internal water particle kinematics based on the previous solutions of η and ϕ.

An essential element of both parts of the BST model lies in its computational efficiency. This is not sought for its own sake, but is an absolute requirement necessary to achieve high resolution in the wavenumber domain, without which realistic broadbanded wave fields cannot be successfully modeled. To optimize the numerical efficiency, the BST model is formulated in terms of the surface parameters, η and $\phi|_{z=\eta}$, where z is the vertical coordinate defined upward from the still water level. This has two overriding advantages. First, it provides a dimensional reduction, and second, it allows both η and ϕ to be represented as Fourier series so that the evaluation of the unknown coefficients can be rapidly achieved using the fast Fourier transform algorithm, and without resource to large matrix inversions.

Unfortunately, with ϕ defined only on the water surface the calculation of $\partial\phi/\partial z$, necessary for the evaluation of the free-surface boundary conditions, requires the application of a Dirichlet–Neumman operator. This problem was tackled by Craig and Sulem (1993) for unidirectional waves, with BST providing an extension to include the effects of directionality. Furthermore, with the adopted Fourier series representation, both η and ϕ must be single-valued functions. As a result, the model can be applied to the description of highly nonlinear waves up to the point of wave breaking, but cannot be used to model overturning waves.

With the fundamentals of the model explained, the only difficulty that remains is the specification of the initial conditions. In essence, this merely involves going back sufficiently far in time, to $t = t_0$, so that the wave field is fully dispersed. With the total wave energy spread across the computational domain there can be no large isolated wave events, and thus both $\eta(x, y, t_0)$ and $\phi(x, y, \eta, t_0)$ can be represented by either a linear or a second-order solution. Further details concerning this essential first step and, in particular, the application of the model to realistic ocean spectra are given in Bateman and Swan (2005, manuscript submitted to *Appl. Ocean Res.*).

3. The spectral response surface method

The SRS method is related to reliability methods that have traditionally been used in structural engineering in order to find the most likely event leading to a response that exceeds the design limitations. This involves three steps:

A: The response of the structure R is defined in terms of a number N of independent, normally distributed, standardized parameters x_n.

B: The value of the response, $R = F$, that meets the design limitations of the structure is calculated, and hence, a *safe* region, $R \leq F$ and a *failure* region, $R > F$, are defined. Figure 1 shows the event space of two variables x_1 and x_2, with each point in the domain representing an event with a certain response $R(x_1, x_2)$. As the parameters have been standardized, the probability density of an event decreases with distance from the origin, β, where $\beta^2 = \Sigma^N x_n^2$. A limit-state surface separates the safe region from the failure region. The value of the response on this surface is a constant, but the probability density (distance from the origin) varies.

C: The design point is the point on the limited-state surface, A, that is the closest to the origin. This has the greatest probability density and, hence, is the failure event that is most likely to occur. The distance of this event from the origin can be utilized to estimate the cumulative distribution function and, hence, the probability of exceedance. This is undertaken through a first- (in a FORM analysis) or second-order (in a SORM analysis) Taylor series expansion of the limited-state surface about the design point.

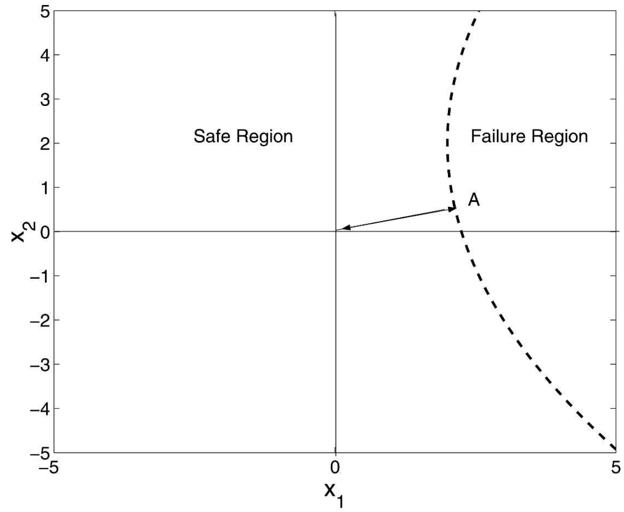

FIG. 1. The response surface for a two-parameter problem, $g(x_1, x_2)$. This surface, denoted by - - -, represents a series of events that have the same values of the response, $R(x_1, x_2)$, but have different probability densities. The response surface separates the safe region from the failure region. Point A is the point closest to the origin; it has the highest probability density and hence is the failure event that is most likely to occur. This corresponds to the so-called design point.

In the present paper the SRS method will be applied to find the point with the greatest response rather than the point with the greatest probability density. This procedure involves three steps:

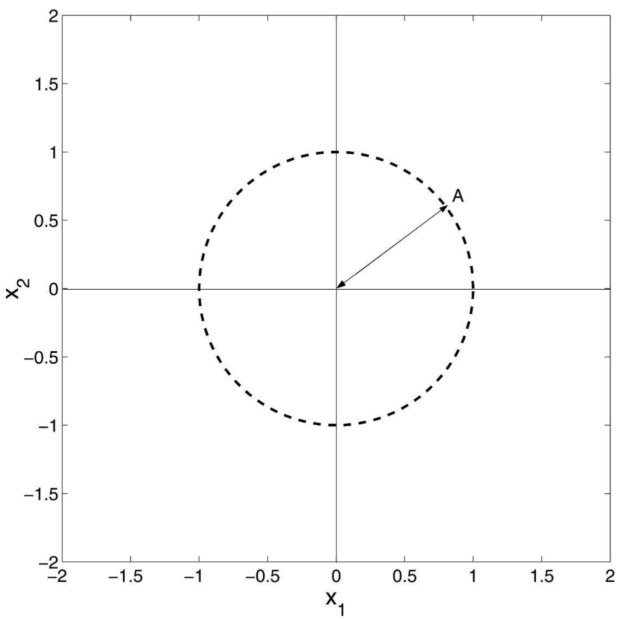

FIG. 2. The response surface representing a series of events that have the same probability density, but different values of response $R(x_1, x_2)$. In this case if A is the point with the highest response it is the design point; $g(x_1, x_2)$ is denoted by - - -.

A: A design spectrum $G_{\eta\eta}(\omega)$ is discretized into a number N of wave components x_n, each of which is statistically independent and normally distributed.

B: The response R (in our case the crest elevation) is defined in terms of these components, and hence, for a certain probability of exceedance a spectral response surface can be described (Fig. 2). On this surface the probability density of each event is constant, but the value of the response varies.

C: The point on this surface with the largest response is determined and its probability of exceedance calculated. The former is achieved by utilizing an optimization routine, the exact nature of which depends upon the manner in which the response function has been defined. The latter is achieved by assuming that the shape of the surface of constant response is either linear (FORM) or parabolic (SORM).

These three steps are described in more detail below.

a. *Discretization of the spectrum (step A)*

The surface elevation $\eta(t)$ at one point in space can be described as the linear sum of many wave components:

$$\eta(t) = \sum_{n=1}^{N} \eta_n = \sum_{n=1}^{N} a_n \cos(\omega_n t - \vartheta_n), \tag{1}$$

where a_n is the amplitude of the nth wave component; ω_n is its circular wave frequency, or $2\pi/T_n$ where T_n is its period; and ϑ_n is a random phase angle. The wave components are statistically stationary, independent variables. Therefore, the variance of each component σ_n^2 can be expressed in terms of the spectral density function $G_{\eta\eta}$ (Ochi 1998):

$$\sigma_n^2 = G_{\eta\eta}(\omega)\Delta\omega, \tag{2}$$

where $\Delta\omega$ is determined by the discretization of the spectrum. The application of the SRS method is simplified by transforming the wave components into standardized variables x_n that all have the same stochastic properties: normally distributed, with zero mean and unit variance,

$$x_n = \frac{\eta_n - \mu_n}{\sigma_n}, \tag{3}$$

where μ_n is the mean value of η_n. Since $\mu_n = 0$ for all n, this simplifies to

$$x_n = \frac{\eta_n}{\sigma_n}. \tag{4}$$

To consider the phasing of the wave components it is necessary to define their Hilbert transform. Since $\eta_n = a_n \cos(\omega_n t - \varphi_n)$, the Hilbert transform $\tilde{\eta}_n$ is given by

$$\tilde{\eta}_n = a_n \sin(\omega_n t - \varphi_n). \tag{5}$$

As $\tilde{\sigma}_n = \sigma_n$, the Hilbert transform of the standardized variable x_n is defined as

$$\tilde{x}_n = \frac{\tilde{\eta}_n}{\sigma_n}. \tag{6}$$

Using these definitions, the amplitude and phase of each component can be expressed in terms of the standardized variables and the standard deviation:

$$\eta_n = \sigma_n x_n = a_n \cos(\omega_n t - \varphi_n), \tag{7a}$$

$$\tilde{\eta}_n = \sigma_n \tilde{x}_n = a_n \sin(\omega_n t - \varphi_n), \tag{7b}$$

$$a_n^2 = (\sigma_n x_n)^2 + (\sigma_n \tilde{x}_n)^2, \quad \text{and} \tag{7c}$$

$$-\varphi_n|_{t=0} = \arctan\left(\frac{\tilde{x}_n}{x_n}\right). \tag{7d}$$

b. *Formulation of the response function (step B)*

To apply the SRS method a response function must be defined. The SRS method can be applied extremely efficiently if this is defined in terms of the standardized variables, x_n and $\tilde{x}_n$. For some responses, such as the response of a structure to nonlinear wave loading (Tromans and Suastika 1998) this can be an extremely difficult task; for other types of response this may be impossible. Examples of the latter include zero-crossing wave height, as it can only be defined in the time domain, and fully nonlinear crest elevation, as it can only be defined from the results of a fully nonlinear wave model. However, a simple example that can easily be defined in terms of the standardized variables is that of the linear crest elevation

$$R = \sum_{n=1}^{N} a_n \cos(\omega_n t - \varphi_n) = \sum_{n=1}^{N} (\sigma_n x_n). \tag{8}$$

c. Calculation of the probability of exceedance (step C)

The probability of exceedance can be calculated by integrating the probability density function over the n-dimensional volume in which the response is greater than the desired crest elevation, C,

$$Q = \iint_{R(x,\tilde{x})>C} \varphi(x, \tilde{x})\, dx\, d\tilde{x}, \tag{9}$$

where Q is the probability of exceedance and φ the probability density function. In terms of structural reliability analysis this is equivalent to integrating the probability density function over the failure region. However, if the surface of constant response is linear (an n-dimensional plane), and the probability density function is given by the Gaussian distribution, then this is given by Hasofer and Lind (1974) in terms of the distance from the origin to the design point, β, as

$$Q_{\mathrm{FORM}} = \Phi[-\beta(x, \tilde{x})], \tag{10}$$

where Φ is the cumulative distribution function. The "design point" is the event with a desired response that is closest to the origin and, hence, has the greatest probability density. In structural engineering the response is defined, the design point found, and the probability of exceedance calculated. In this paper, the probability of exceedance will be defined, the design point found, and the response associated with that probability calculated. Equation (11) describes the response surface $g(x_n, \tilde{x}_n)$, that is a n-dimensional "sphere" in the space of the standardized variables, x_n and $\tilde{x}_n$:

$$g(x_n, \tilde{x}_n) = \sum_n x_n^2 + \sum_n \tilde{x}_n^2 = \beta^2. \tag{11}$$

As all the variables are standardized, the sphere represents points with an equal probability density. The maximum response on this surface defines the design point and can be found through a standard optimization routine (Press et al. 1994). Once the design point has been identified, the probability of exceedance of the response can be calculated. As this paper is concerned with the probability of exceedance of crest elevation, rather than of surface elevation, this is approximated for large crests by the Rayleigh distribution

$$Q_{\mathrm{FORM}} = P[C > R(x, \tilde{x})] = \exp\left[-\frac{\beta(x, \tilde{x})^2}{2}\right]. \tag{12}$$

The validity of this approximation is discussed in reference to linear wave theory by Longuet-Higgins (1952), who built on the work of Rice (1944, 1945). However, the use of the Rayleigh distribution for nonlinear crest elevation relies on the assumption that large crests form from the focusing of many small wave components. This assumption implicitly neglects the possibility of large waves emerging from the modular instability of a regular wave train. However, the authors firmly believe that such waves are not characteristic of the largest waves in a deep-water broadbanded sea state and that the Rayleigh distribution is entirely appropriate. This is discussed in more detail in section 4.

If the surface of constant response is nonlinear then the estimation of the probability of exceedance can be improved by considering the surface to be parabolic rather than linear. This is achieved by considering the Taylor series expansion of the surface about the design point, a full description of which can be found in Madsen et al. (1986) and Melchers (1987). In the present investigation, the SORM analysis is simply applied to determine the importance of the shape of the response surface. To this end, if it is assumed that a Rayleigh distribution is equally applicable to a SORM analysis then it follows that in the space of two variables x_1 and x_2 the probability of exceedance is given by

$$Q_{\mathrm{SORM}} = \int_{-\infty}^{\infty} \int_{x_2=C}^{x_2=\infty} \frac{\exp(-x_1^2/2)}{(2\pi)^{1/2}} x_2 \exp(-x_2^2/2)\, dx_2\, dx_1, \tag{13}$$

where $C = \beta - 0.5\, \kappa x_1^2$ is the surface of constant response, and therefore

$$\begin{aligned} Q_{\mathrm{SORM}} &= \int_{-\infty}^{\infty} \frac{\exp(-x_1^2/2)}{(2\pi)^{1/2}} \exp[-(\beta^2 - \kappa\beta x_1^2 \\ &\quad + 0.25\kappa^2 x_1^4)/2]\, dx_1 \\ &\approx \exp(-\beta^2/2) \int_{-\infty}^{\infty} \frac{\exp(-x_1^2/2)}{(2\pi)^{1/2}} \exp(\kappa\beta x_1^2/2)\, dx_1. \end{aligned} \tag{14}$$

Therefore, for N components

$$Q_{\mathrm{SORM}} = Q_{\mathrm{FORM}} \prod_n^{N-1} (1 - \beta\kappa_n)^{-1}, \tag{15}$$

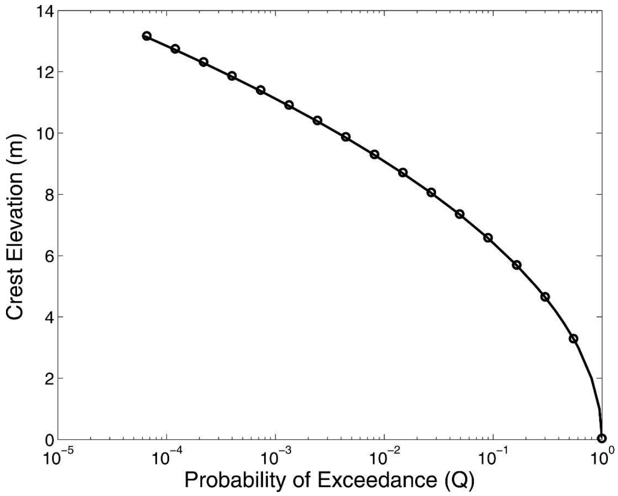

FIG. 3. Probability of exceedance of crest elevation, for case J1. Comparison between the statistics calculated by using the SRS method with a linear response function (—) and those of the Rayleigh distribution (○).

where κ_n are the principal curvatures of the surface of constant response,

$$\kappa_n = -\frac{\partial^2 y_N}{\partial y_n^2}, \tag{16}$$

and where the vectors y_n are orthogonal to the vector of the design point y_N and can be found by applying a method of singular value decomposition (Press et al. 1994).

In the next section the probability of exceedance of crest elevation will be calculated for two unidirectional spectra. To achieve this, a number of response surfaces, or n-dimensional spheres, must be generated. Each sphere will have a different radius and will therefore represent a different probability of exceedance. These response surfaces will be searched in turn and in each case the point of maximum response found. Hence, the maximum crest elevation with a certain probability of exceedance will have been calculated. Figure 3 shows that if this is undertaken using the response function of linear crest elevation [Eq. (8)] the results are, not surprisingly, in perfect agreement with those of the Rayleigh distribution.

Up to this point the calculations have all been undertaken in the probability domain. However, it is also possible to determine the time history of water surface elevation associated with the most probable event corresponding to a particular response. This can be achieved through the use of Eqs. (7a)–(7d). If the response function is defined by linear crest elevation, the profiles of the most probable events are, as expected, identical to those given by Lindgren (1970), Boccotti (1983), and, more recently, the NewWave theory of Tromans et al. (1991). In this case, the wave profile corresponds to the scaled autocorrelation function of the underlying random process.

4. Fully nonlinear wave statistics

In the following section two unidirectional spectra have be investigated: case J1 and case J5. Both are Joint North Sea Wave Project (JONSWAP) spectra of significant wave height $H_s = 12$ m and peak period $T_p = 12.8$ s, the former having a peak-enhancement factor $\gamma = 1$ and the latter $\gamma = 5$. The spectral shape determines the variance of each wave component and hence defines the probability that a wave component will have a particular amplitude. Therefore, it is possible that in the optimization process a different wave spectrum will be selected. The *optimized* spectrum represents one possible event that could occur, with the probability of it occurring determined by the statistics of the underlying wave field. The optimization process selects this event as the most probable profile for a given probability of exceedance, in this case crest elevation.

Tromans and Vanderschuren (2004) applied the SRS method using both a linear and a second-order response function, both calculated using a FORM. They found that if the linearly optimized spectrum is used as the input to the second-order model of Sharma and Dean (1981), the crest elevations are almost identical to the results of the second-order optimization. This reflects the fact that the spectra optimized to second order are very similar to those optimized to first order. This result was, perhaps, to be expected since while the spectra optimized using the second-order response function do not include the second-order, sum and difference bound waves, they have been optimized on the basis that these waves exist. As bound waves cannot alter the phasing or the amplitude of the linear, freely propagating wave components, their effect is limited by the second-order kernel, which has been plotted for two wave components by Forristall (2000). The SRS method, with a second-order response function, optimizes the amplitude of the wave components (the shape of the spectrum) so that the combined contribution from the linear terms and the second-order kernel produces the greatest crest elevation. However, the optimization is constrained such that the probability of exceedance of the wave spectrum must equal a desired value. Hence, any increase in the crest elevation associated with the second-order terms is correlated with a reduction in the crest elevation associated with the linear terms. In this case the balance is weighted toward the latter, and the result is that the spectra optimized to second order are similar to those optimized linearly. Put simply, in a realistic sea state the second-order increase in crest elevation is insensitive to the exact shape of the spectrum.

On the other hand, if the full nonlinearity of the wave field is modeled, the resonant and near-resonant interactions arising at the third and higher orders of the wave steepness become significant, and these can lead to rapid changes to the wave spectrum in the vicinity of the large wave event (GS). With the underlying linear wave field providing the input to the fully nonlinear wave model, calculations are based upon the assumption that high crests arise from the focusing of wave components. However, as these wave components begin to focus they interact in such a way that the design event occurs. This interaction is modeled fully nonlinearly and may result in the amplitudes and phases of the wave components changing. This nonlinearity is captured in the position and the shape of the surface of constant response when constructed in the space of the initial linear input. In unidirectional seas these interactions can lead to large increases in crest elevation, and in contrast to the second-order interactions, they *are* sensitive to the shape of the initial spectrum. Indeed, the near-resonant interactions that dominate the evolution of a unidirectional spectrum can only occur for wave components that are closely spaced (Benjamin and Feir 1967). Therefore, it might be expected that there will be a significant difference between the nonlinear response that results from a spectrum that has been optimized linearly with one that has been optimized fully nonlinearly. These two methods of obtaining a response are labeled the *correction* method and the *exact* method, respectively. In the former the spectra are optimized linearly, and the resulting spectrum used as the input to the fully nonlinear wave model, BST. This yields an underprediction of the actual response. In contrast, in the latter the spectra are optimized fully nonlinearly by incorporating the BST model within the SRS method.

a. The correction method

In this section the fully nonlinear wave model has been applied to the linearly optimized spectra of cases J1 and J5 in order to calculate fully nonlinear crest elevations by the correction method. Figure 4 indicates that the effect of including the full nonlinearity is significant, with an increase in crest elevation of over 1 m for near-breaking waves with probabilities of exceedance $Q < 0.05$. Furthermore, the results show that a

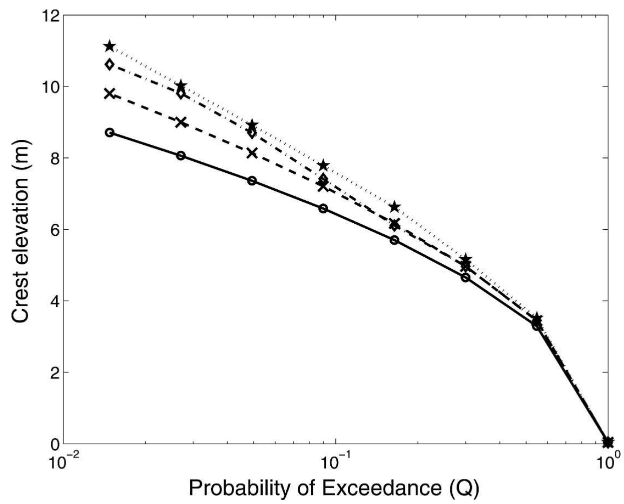

FIG. 4. Probability of exceedance of crest elevation calculated by the fully nonlinear correction method for cases J1 and J5, where (-○-) denotes linear (identical results for both case J1 and case J5), (- × -) second-order case J5 (similar results for case J1), (-·- ◇ -) fully nonlinear case J1, and (· ★ ·) fully nonlinear case J5.

reduction in the spectral bandwidth, corresponding to an increase in the peak-enhancement factor, leads to larger maximum crest elevations (case J5). However, the results of these calculations should be treated with caution because the spectra have not been optimized fully nonlinearly. Indeed, to ascertain the accuracy of the correction method and, hence, the extent to which it underpredicts the crest elevation associated with a particular probability of exceedance, the statistics must also be calculated using the exact method.

b. The exact method

To apply the exact method the nonlinear wave model, BST, must be incorporated into the implementation of the SRS method so that the response function is determined by the results of the wave model. To achieve this, the wave model must be run once to determine the response associated with any single event, the desired output being the maximum crest elevation within that particular run. To identify the event that has the largest response on a particular surface, the BST model must be run many times. Although the wave model is highly efficient, individual runs typically take one hour. The overall time taken then depends upon the nonlinearity of the wave field and the number of components into which the spectrum is discretized. In the present cases the discretization involves 100 pairs of wave components (x_n and $\tilde{x}_n$), and the computations took several days to calculate the crest elevations associated with each probability of exceedance. While in

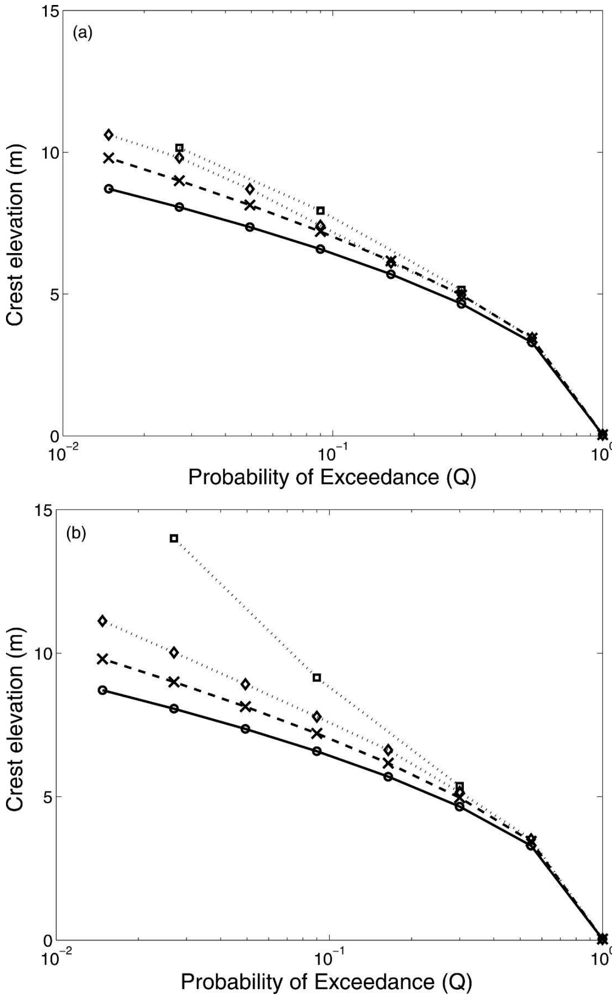

FIG. 5. Comparison between the probability of exceedance of crest elevation calculated by the correction and the exact methods for (a) case J1 and (b) case J5, where (-○-) denotes linear, (- × -) second-order, (· ◇ ·) correction, and (· □ ·) exact.

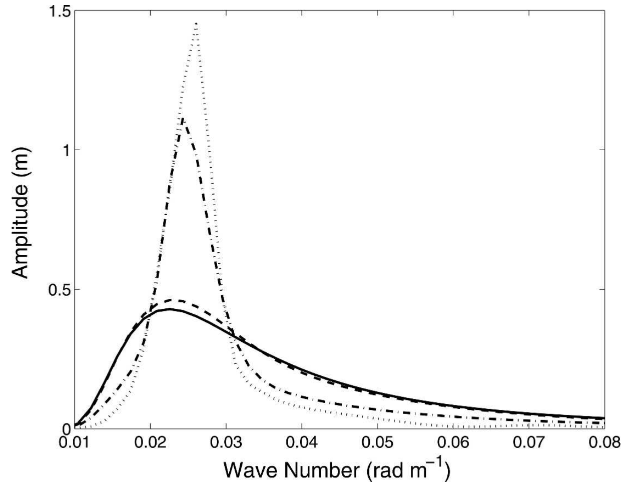

FIG. 6. Spectra of cases J1 and J5 optimized fully nonlinearly, where (—) denotes J1 optimized linearly, (- - -) J1 optimized fully nonlinearly, (- · · -) J5 optimized linearly, and (· · ·) J5 optimized fully nonlinearly.

unidirectional sea states it is time consuming to optimize a spectrum fully nonlinear, in directional sea states many more wave components are required and the calculations take several weeks to identify the crest elevation for a given probability of exceedance. It is for this reason that only unidirectional sea states have been considered in this paper. A different approach is presently under development in order to optimize directional spectra and will be discussed in a future paper.

Owing to the length of time it takes to optimize a spectrum fully nonlinearly, only a limited number of points have been included for each wave case. Nevertheless, the trends indicated on Fig. 5 are clear. In narrowbanded sea states the fully nonlinear optimization of the wave spectrum leads to a significant increase in the crest elevation. For example, in case J5 the increase in crest elevation is greater than 3.3 m for a probability of exceedance defined by $Q = 0.027$, where the latter value corresponds to a 92% chance of this event being exceeded in 20 min of a storm. However, in more broadbanded sea states the increase is much less significant: in case J1 the increase is only 0.5 m for $Q = 0.027$. These results suggest that, in unidirectional sea states, narrowbanded spectra give rise to larger nonlinear increases in crest elevation, indicating that such sea states can be considered more nonlinear. This is entirely consistent with the laboratory observation of extreme wave groups reported by Baldock et al. (1996). Further evidence of this is given by the shape of the optimized spectra shown in Fig. 6: in both cases J1 and J5 an increase in crest elevation is associated with a narrowing of the wave spectrum, the effect being more pronounced in the latter case.

The application of the exact method not only optimizes the amplitudes of the wave components, but also their relative phasing. In a linear or second-order analysis this is unnecessary because it is possible to predict the time and location of a focused wave using the linear dispersion relationship. However, third- and higher-order nonlinear interactions are capable of altering the dispersive properties of the wave components and hence the focal quality of the design event. This effect explains part of the difference between crest elevations calculated using the correction method and those calculated using the exact method. However, it has been found that changes to the focal quality of the event are much less important than changes to the bandwidth of the wave spectrum.

c. Second-order reliability method

In the previous sections the probability of exceedance has been calculated using a first-order reliability method, and hence, the calculations have been undertaken assuming that the surface of constant response is linear. Therefore, while the application of the SRS method has considered the nonlinearity of the response, it has not considered the nonlinearity of the response surface. In this section a second-order reliability method will be applied in order to ascertain what effect the assumption that the response surface is linear has on the statistics of crest elevation.

For the probability of exceedance to be calculated using a second-order reliability method the curvature of the response surface must be ascertained along vectors perpendicular to that of the design point [Eq. (16)]. If this curvature is positive the size of the "failure" region will be overestimated and the probability of exceedance calculated using a first-order reliability method will be an overprediction; conversely, if it is negative the probability of exceedance will be underpredicted.

If the response function was given explicitly, calculating the curvature would be a straightforward task; however, for the response of fully nonlinear crest elevation the response surface must be calculated from the results of the numerical wave model. This has been undertaken by considering the Taylor series expansion of the response surface about the design point, in the plane of two vectors y_i and y_N:

$$R(y_i, y_N) = R_0 + \frac{\partial R}{\partial y_i}\Delta y_i + \frac{\partial R}{\partial y_N}\Delta y_N + \frac{1}{2}\frac{\partial^2 R}{\partial y_i^2}(\Delta y_i)^2 + \frac{1}{2}\frac{\partial^2 R}{\partial y_N^2}(\Delta y_N)^2 + \frac{1}{2}\frac{\partial^2 R}{\partial y_N \partial y_i}\Delta y_N \Delta y_i, \quad (17)$$

where R_0 is the response at the design point.

By calculating the response along the various orthogonal vectors, and curve fitting a parabola to these results, it is possible to calculate all of the gradients in Eq. (17) except the cross product $\partial^2 R/\partial y_i \partial y_N$. As an example, Fig. 7 shows the change in the response along three particular vectors: the first is the vector of the design point, y_N, with the small periodic oscillations the result of *resonant* changes to the phasing of the wave components, the second is a vector that has very little curvature and is typical of most of the results, whereas the third is a vector along which the curvature of the response is relatively large. Once the response along every orthogonal vector has been established it is possible to use Eq. (17) to calculate the equation of the surface of constant response in the plane of y_N and y_i as

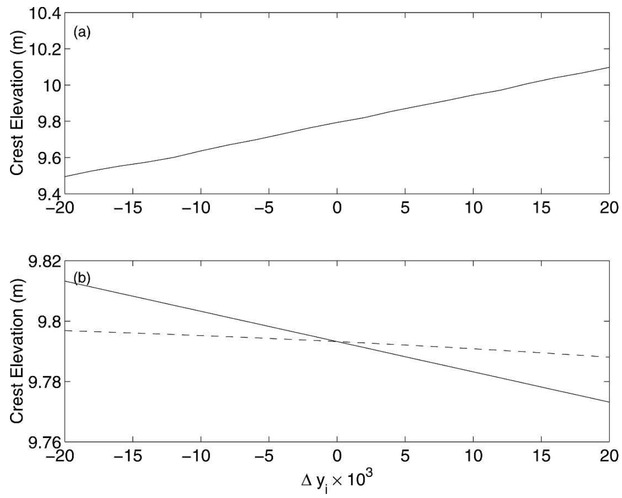

FIG. 7. Changes in the value of the fully nonlinear response of case J5 (a) along the vector of the design point and (b) along two vectors orthogonal to the design point, where (—) denotes typical vector with very little curvature, and (- - -) denotes vector with relatively "large" curvature.

$$\frac{\partial R}{\partial y_i} y_i + \frac{\partial R}{\partial y_N} y_N + \frac{1}{2}\frac{\partial^2 R}{\partial y_i^2} y_i^2 + \frac{1}{2}\frac{\partial^2 R}{\partial y_N^2} y_N^2 = 0, \quad (18)$$

where the cross-product term has been neglected. Differentiation of this gives the curvature of the response surface as

$$\frac{\partial^2 y_N}{\partial y_i^2} = -\frac{\left[m_4\left(\frac{m_1}{m_2}\right)^2 + m_3\right]}{m_2}, \quad (19a)$$

where

$$m_1 = \frac{\partial R}{\partial y_i},$$

$$m_2 = \frac{\partial R}{\partial y_N},$$

$$m_3 = \frac{\partial^2 R}{\partial y_i^2}, \quad \text{and}$$

$$m_4 = \frac{\partial^2 R}{\partial y_N^2}. \quad (19b)$$

Having calculated the curvature of the response surface it is possible to apply Eq. (15) and to calculate the change in the probability of exceedance due to the nonlinearity of the response surface. For case J5 and a probability of exceedance $Q_{\mathrm{FORM}} = 0.09$, the response surface is convex. This suggests the first-order calculation of the probability of exceedance is an overprediction, with $Q_{\mathrm{SORM}} = 0.087$. Therefore, the second-order

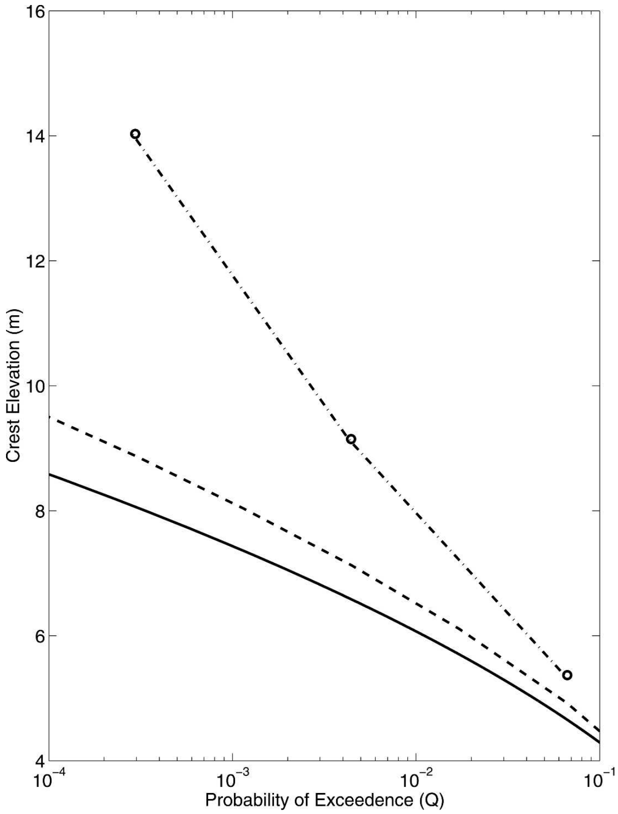

FIG. 8. Comparison between the probability of exceedance calculated using a first- and second-order reliability method, where (—) denotes linear, (- - -) second order, (○) fully nonlinear FORM calculation, and (- · -) fully nonlinear SORM calculation.

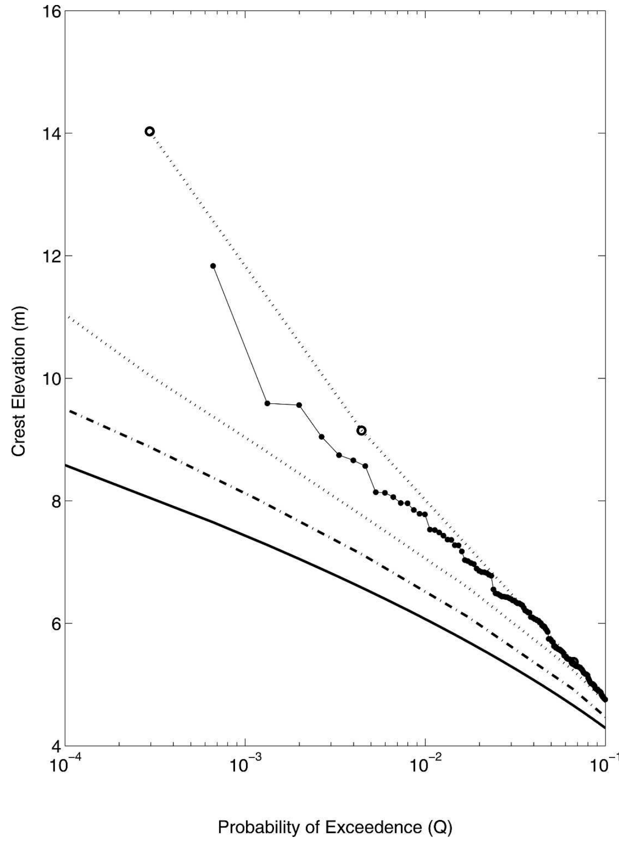

FIG. 9. Comparison between the results of the SRS method and fully nonlinear time-domain simulations for case J5, where (—) denotes linear, (- · -) second order, (· · ·) fully nonlinear correction method, (·○·) fully nonlinear exact method, and (—●—) fully nonlinear time-domain simulations.

analysis results in only a very slight reduction of the probability of exceedance, of the order of 3.5%, which indicates that the response surface is almost linear. Indeed, following a large number of tests, it has been concluded that the nonlinearity of the response function is much more important than the nonlinearity of the response surface. To highlight this conclusion, Fig. 8 shows a comparison between the results of the first-order reliability analysis and those of the second-order reliability analysis, with a reduction in the probability of exceedance of approximately 3.5% barely noticeable on the log scale.

5. Fully nonlinear time-domain simulations

In an attempt to validate the present results, fully nonlinear time-domain simulations have been undertaken for case J5. This has been achieved by initializing BST with a random realization of the desired spectrum with $H_s = 8$ m. BST has been run 10 times for 4000 s and the surface elevation has been recorded at one point in the spatial domain of length 40 000 m. While this might be expected to correspond to approximately 3000 waves, only 1500 have been obtained. The reason for this discrepancy is that the wave model can only simulate the evolution of a wave field up to the point at which a wave breaks. Therefore, in the realizations of the random sea state that contain the largest waves the fully nonlinear simulation has terminated before the entire 4000 s of data have been collected. This inevitably means that there are fewer waves associated with large sea states and hence has implications for the statistics of crest elevation derived from the fully nonlinear simulations. This is an inherent difficulty in collecting wave statistics using such a model. Nevertheless, individual waves within the resulting time traces, $\eta(t, x = 0)$, have been separated by their zero up-crossings and their crest elevations calculated.

Figure 9 shows that the fully nonlinear application of the SRS method is in good agreement with statistics derived from the time-domain simulations. In particular, it is clear that any discrepancies are small in com-

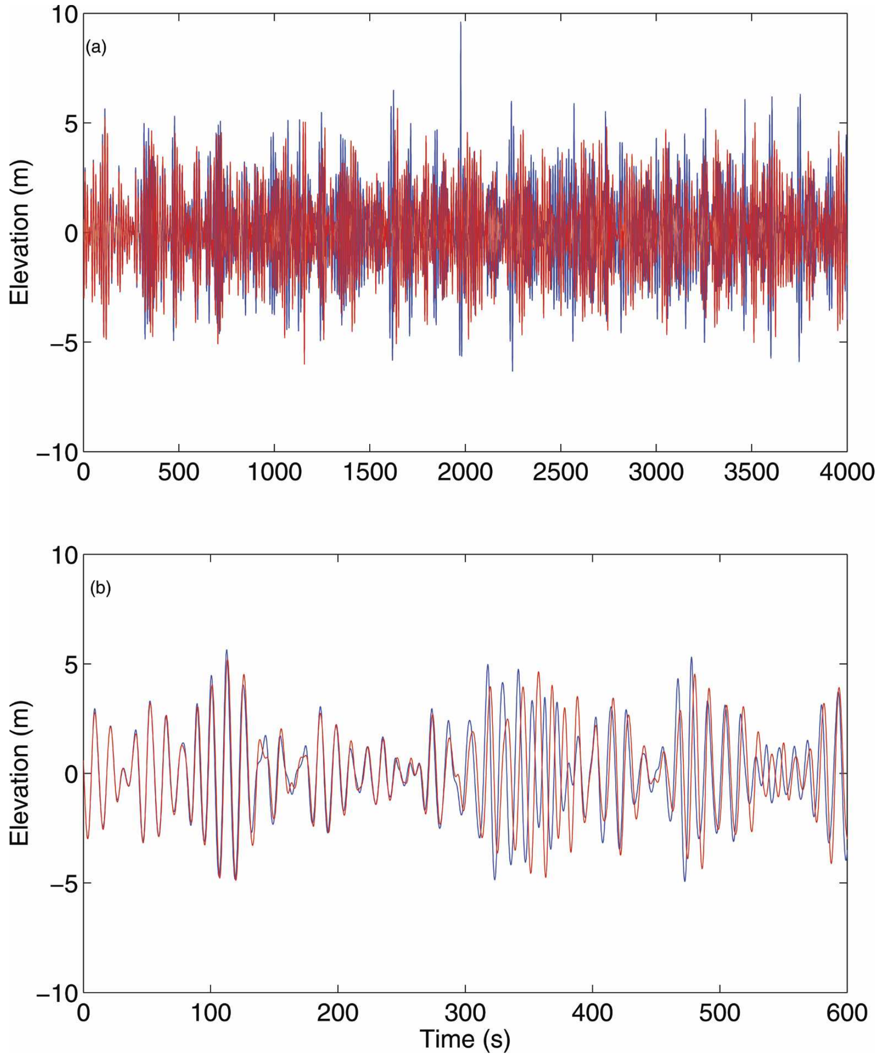

FIG. 10. Comparison between a linear and a fully nonlinear random realization of case J5: (a) $0 \leq t \leq 4000$ s and (b) $0 \leq t \leq 600$ s, where the blue solid line denotes fully nonlinear and the red solid line denotes linear.

parison with the difference between the time-domain results and the linear or second-order theory. Despite the general agreement between the SRS method and the time-domain simulations, the former slightly overpredicts the crest elevations. This is surprising, as the main limitation of the SRS method is that the optimization process may not have found the largest response for a particular probability of exceedance. Therefore, it would be expected to underpredict crest elevations. There are at least three reasons for discrepancies between the two approaches. The first, and probably the most significant, is that the time-domain simulations cease when a wave breaks, and hence there are fewer data from the realizations of the largest sea states. The second arises because the fully nonlinear simulations based on the SRS method assume that the results obtained from a fully dispersed wave group focusing together on an otherwise calm sea are representative of the same group forming, at least on average, in the presence of a random background. Early theoretical work, notably by Alber (1978), but with other contributions reviewed by Yuen and Lake (1982), has suggested that the random background may partially disrupt the dominant third-order interactions accounting for the increased crest elevations. However, the results typically concern very narrowbanded spectra, modeled using the nonlinear Schrodinger equation, and may not be relevant to the sea states considered herein. Indeed, separate calculations have been undertaken to examine the effects of a random background, and, so far, it has been found to be relatively unimportant; however, this work remains ongoing. The third reason is that the sea state modeled in the time-domain simulations is nonstationary: not only are there rapid changes to the spectrum that are associated with large wave events, but also more gradual changes associated with smaller events. Both of these changes are the result of the near-resonant interactions described by Benjamin and Feir (1967). However, after the formation of a focused event these interactions reverse and so there are no significant changes to the wave spectrum. In contrast, the presence of waves that are not focused leads to gradual changes to the spectrum, and hence the comparisons with the current application of the SRS method cease to be compatible.

A direct comparison between the linear and fully nonlinear random wave profile is shown in Fig. 10, the lower panel of which depicts the first 600 s of one particular random realization. In this figure not only are the fully nonlinear crest elevations significantly higher than those predicted using linear theory, but they also occur earlier, with the latter effect attributed to changes to both the wave spectrum, and also nonlinear changes in the phase speed. What is also noticeable is that, apart from second-order nonlinearities, which sharpen the peaks and broaden the troughs, the two profiles are in good agreement until the occurrence of the large wave group at $t \approx 320$ s. On its own this is certainly not conclusive, but it supports the notion that the formation of a large wave coincides with rapid changes to the wave spectrum, as discussed in GS.

In effect, these comparisons confirm that the nonlinearity of a wave field leads to two types of spectral changes: those that are both local and rapid, that depend on the evolution of individual wave groups, and those that evolve over much longer time-scales involving hundreds or perhaps thousands of wave cycles. While these two types of spectral evolution may represent the same physical process, namely, third-order *near-resonant* interactions (GS), they can have a very different effect on the statistics of crest elevation. The present approach, incorporating a nonlinear wave model (BST) within the SRS method, includes the former, but not the latter, and in so doing remains consistent with the concept of a design spectrum. Indeed, it is important to stress that the inclusion of the latter involves the solution of a more complicated problem in which any notion of a design spectrum becomes inappropriate. Furthermore, a solution of this problem would have to include not only the nonstationary nature of wave-modulation effects, but also that of energy input and dissipation within a developing sea state.

6. Conclusions

The statistics of crest elevation have been calculated by incorporating a fully nonlinear wave model into the spectral response surface method. The results have been shown to be in good agreement with fully nonlinear time-domain simulations. The statistics have shown that in unidirectional seas, particular those that are narrowbanded, crest elevations can be much higher than would be predicted by linear or second-order theory. Although completely unidirectional seas are unrealistic, the presence of locally long crested sea states offers an explanation as to the occurrence of freak, or rogue, waves in deep water.

Acknowledgments. The early stages of this work were undertaken within the project "Reliability Based Structural Design of FPSO Systems," which involves Shell, Instituto Superior Tecnico, DHI, Det Norske Veritas, Imperial College, Noble Denton, and Oxford University. The project is partially funded by the European Union through the Energy Programme under Contract ENK6-2000-00107. The later stages of the work were completed with support from the U.K. Engineering and Physical Sciences Research Council under Grant GR/R64971.

REFERENCES

Alber, I., 1978: The effect of randomness on the stability of two-dimensional surface wave trains. *Proc. Roy. Soc. London,* **363A,** 525–546.

Baldock, T. E., C. Swan, and P. H. Taylor, 1996: A laboratory study of nonlinear surface waves on water. *Philos. Trans. Roy. Soc. London,* **354A,** 649–676.

Bateman, W. J. D., C. Swan, and P. H. Taylor, 2001: On the efficient numerical simulation of directionally spread surface water waves. *J. Comput. Phys.,* **174,** 277–305.

——, ——, and ——, 2003: On the calculation of the water particle kinematics arising in a directionally spread wavefield. *J. Comput. Phys.,* **186,** 70–92.

Benjamin, T. B., and J. E. Feir, 1967: The disintegration of wavetrains on deep water. *J. Fluid Mech.,* **27,** 417–430.

Boccotti, P., 1983: Some new results on statistical properties of wind waves. *Appl. Ocean Res.,* **5,** 134–140.

Craig, W., and C. Sulem, 1993: Numerical simulation of gravity waves. *J. Comput. Phys.,* **108,** 73–83.

Forristall, G. Z., 2000: Wave crest distributions: Observations and second-order theory. *J. Phys. Oceanogr.,* **30,** 1931–1943.

Gibson, R. S., and C. Swan, 2007: The evolution of large ocean waves: The role of local and rapid spectral changes. *Proc. Roy. Soc. A,* **463,** 21–48.

Hasofer, A. M., and N. C. Lind, 1974: Exact and invariant second-moment code format. *J. Eng. Mech. Div.,* **100,** 111–121.

Lindgren, G., 1970: Some properties of a normal process near a local maximum. *Ann. Math. Stat.,* **41,** 1870–1883.

Longuet-Higgins, M. S., 1952: On the statistical distribution of the heights of sea waves. *J. Mar. Res.,* **11,** 245–266.

Madsen, H. O., S. Krenk, and N. C. Lind, 1986: *Methods of Structural Safety.* Prentice Hall, 403 pp.

Melchers, R. E., 1987: *Structural Reliability Analysis and Prediction.* Ellis Horwood, 400 pp.

Ochi, M. K., 1998: *Ocean Waves: The Stochastic Approach.* Cambridge University Press, 319 pp.

Press, W. H., B. P. Flannery, S. A. Teukolsky, and W. T. Vetterling, 1994: *Numerical Recipes in C—The Art of Scientific Computing.* Cambridge University Press, 994 pp.

Rice, S., 1944: Mathematical analysis of random noise. *J. Bell Syst. Technol.,* **23,** 282–332.

——, 1945: Mathematical analysis of random noise (continued). *J. Bell Syst. Technol.,* **24,** 46–156.

Sand, S., 1990: Freak wave kinematics. *Water Wave Kinematics,* A. Tørum and O. T. Gudmestad, Eds., Kluwer Academic, 535–550.

Sharma, J. N., and R. G. Dean, 1981: Second-order directional seas and associated wave forces. *Soc. Petrol. Eng. J.,* **4,** 129–140.

Tromans, P. S., and I. K. Suastika, 1998: Spectral response surfaces, designer waves and the ringing of offshore structures. *Proc. OTRC Symp.: Ocean Wave Kinematics, Dynamics and Loads on Structures,* Houston, TX, American Society of Civil Engineers, 171–178.

——, and L. Vanderschuren, 2004: A spectral response surface method for calculating crest elevation statistics. *J. Offshore Mech. Arct. Eng.,* **126,** 51–53.

——, A. Anaturk, and P. Hagemeijer, 1991: A new model for the kinematics of large ocean waves—Application as a design wave. *Proc. First Offshore and Polar Engineering Conf. (ISOPE),* Edinburgh, United Kingdom, International Society of Offshore and Polar Engineers, 64–71.

Yuen, H. C., and B. M. Lake, 1982: Nonlinear dynamics of deep-water gravity waves. *Adv. Appl. Mech.,* **22,** 67–229.

Zakharov, V. E., 1968: Stability of periodic waves of finite amplitude on the surface of a deep fluid. *J. Appl. Mech. Tech. Phys.,* **9,** 190–194.